This article has been accepted for publication in a future issue of this journal, but has not been fully edited. Content may change prior to final publication. Citation information: DOI 10.1109/TSG.2017.2695196, IEEE Transactions on Smart Grid

Improved Battery Storage Valuation Through Degradation Reduction

Brandon Foggo, *Student Member, IEEE* and Nanpeng Yu, *Senior Member, IEEE*

***Abstract*—The widespread adoption of battery energy storage systems (BESS) has been hindered by the uncertainty of their financial value. In past research, this value has been estimated by optimizing the system's actions over the course of the battery's lifetime. However, these estimates did not consider the fact that battery actions decrease the lifetime itself. This paper uses realistic battery cycle degradation to re-evaluate BESS profitability and attempts to increase profits by mitigating this degradation. For this purpose, the paper develops an approximate linear model of degradation suitable for co-optimization with the set of battery actions. It is shown through simulation that 29.1% of the storage system's value is lost because of cycle degradation. However, co-optimization through the approximate model reduces this loss to just 3.3%.**

***Index Terms*—Batteries, Degradation, Economics, Optimization, Valuation**

NOMENCLATURE

Section III-A

$\mathbf{A}$	Matrix of revenues [$\$/MW$].
E_{max}	Maximum State of Charge [MWh].
LMP	Locational marginal price [$\$/MW$].
N	Number of optimization steps [$steps$].
O	Operation and maintenance costs [$\$/MW$].
P_{max}	Maximum power output [MW].
Reg^d	Revenue for committing 1 MW of capacity for regulation down [$\$/MW$].
Reg^u	Revenue for committing 1 MW of capacity for regulation up [$\$/MW$].
S	Battery State of Charge [MWh].
T	Number of hours per optimization step [hrs].
$\mathcal{T}$	Estimated battery lifetime [hrs].
d	Discharged power output [MW].
n	Optimization step index [$steps$].
p^u, p^d	Proportion of capacity committed to regulation up/down that is called upon in real time operations [unitless].
r^u, r^d	Committed capacity for regulation up/down [MW].
t	Hour index [hrs].
$\mathbf{x}$	Vector of decision variables [mixed].
γ	Battery self-discharge rate [unitless].
κ	Battery cycle efficiency [unitless].
ρ	Battery resistive loss factor [unitless].

Section III-B

CR	Cycle Current Rate [MW / unitless].
DoD	Cycle Depth of Discharge [MWh / unitless].
SoC	Cycle mean State of Charge [MWh / unitless].
deg	Degradation rate [unitless].
f	Regulation signal [unitless].
f^u, f^d	Positive/negative part of the regulation signal [unitless].
i	Cycle index [$cycles$].
k	Intra-hour tick index [$ticks$].

Section IV

$\mathcal{I}$	SoC Bounding Region [MWh].
R	Normalized half length of $\mathcal{I}$ [unitless].
ψ	State of Charge continuous time approximation [MWh].
ψ_m, ψ_M	High/low frequency component of ψ [MWh].
τ	Continuous time index [hrs].

Section V

$\mathbf{A}'$	Modified matrix of revenues [$\$/MW$].
J_{CR}	Current Rate Constant [unitless].
J_{SoC}	SoC Constant [unitless].
M^{deg}	Linear degradation multiplier [$].
U_z	Set of hours in which the low frequency profile is flat [unitless].
X	Approximated hourly degradation [unitless].
a_1, a_2	Micro/macro cycle linearization constant [unitless].
$\mathbf{b}$	vector of multipliers for linear degradation [$1/MW$].
c'	auxiliary charging decision variable [MW]
d'	auxiliary discharging decision variable [MW]
p_z	Probability that the low frequency profile is flat [unitless].
$\mathbf{x}'$	Modified decision vector [mixed].
μ	1-dimensional conditional cycle counting measure on DoD intervals [$cycles$].
μ_m, μ_M	Micro/macro decomposition of μ [$cycles$].
ν	2-dimensional cycle counting measure on DoD $\times$ SoC rectangles [$cycles$].
ϕ	Nonlinear functional to obtain total depth of discharge from a continuous function [unitless].
$\tilde{\psi}$	Augmented SoC profile [MWh].
σ_u^2, σ_d^2	Regulation signal up and down variances [unitless].

B. Foggo is with the University of California, Riverside (email: bfogg001@ucr.edu)

N. Yu is with University of California, Riverside

This article has been accepted for publication in a future issue of this journal, but has not been fully edited. Content may change prior to final publication. Citation information: DOI 10.1109/TSG.2017.2695196, IEEE Transactions on Smart Grid

I. Introduction

Renewable power generation is quickly making its way into the electric power grid. With it comes the stochastic nature of the sources that drive it. Stochastic generation complicates the act of balancing power generation and load. With fast ramping rates and the ability to dynamically switch between power generation and absorption, battery energy storage systems (BESS) mitigate this challenge. However, the profitability of doing so remains under question.

BESS owners can profit through the actions of energy arbitrage and providing one or more of the ancillary services described in [1]. While much research has been done on the value of BESS systems directly linked to renewable sources [2] [3], for energy arbitrage [4], and for primary frequency regulation [5], a large amount of the existing literature has underestimated potential profits by failing to optimize these actions simultaneously. By correcting these issues, [6] and [7] obtained a significantly more optimal valuation of BESS. However, this result was obtained by considering only the effect of time on the battery's deterioration. But any analysis which does not consider the impact of battery charging actions on degradation will likely overestimate the value of the battery because the battery will degrade faster than the modeling suggests.

It is reasonable to believe that co-optimization of degradation with energy arbitrage and ancillary services should significantly mitigate the loss in BESS value from cycle degradation. Such co-optimization is the goal of this paper. Unfortunately, current degradation models are not suitable for this coupled optimization because their dependence on battery actions is calculated by a series of complicated, non-injective, and, most importantly, non-closed form transformations.

In this paper, we will develop an accurate analytical approximation of cycle degradation suitable for the search space in question. We will then use this model to compute the value of a BESS co-optimized over battery actions (arbitrage and regulation services) and cycle degradation. The use of co-optimization with this model results in a profit increase of 36% over the non co-optimized case.

The rest of this paper is organized as follows. Section II provides a literature review on existing degradation models and the optimization use cases upon which they are suitable. Section III describes the process of energy storage valuation with realistic degradation that is not co-optimized with the battery actions. Section IV lists a set of properties evident in the valuation framework that will be used to linearize the degradation calculation. Section V derives the linearization. Numerical evaluations and the performance of the degradation model will be presented in section VI. Conclusions will be made in section VII.

II. Literature Review

Only a few attempts have been made to couple a BESS ancillary service optimization problem with degradation. However, there is research in degradation models suitable to other optimization use cases.

Reference [8] introduces one of the lowest level degradation models suitable for application. The model considers a current driven differential equation representing build up of resistance at the battery anode. This is coupled with a low level battery discharge model to find the driving current. The model was used to find optimal charging schemes for electric vehicles. Since it is such a low level model, it is difficult to use in more complicated optimization schemes. It also only considers resistive build up, and thus does not consider capacity loss. Nonetheless, if the optimization use case is based directly on charging and discharging profiles with little uncertainty, then this is a good model with excellent theoretical justification.

Most models describe degradation in terms of cycling parameters. Reference [9] provides a comprehensive, test driven analysis of battery degradation based on these parameters. It includes analysis in both capacity loss and resistive build up. The paper does not provide an analytical model for degradation, but does discuss useful insights for the effects of each cycle parameter of degradation. These insights can be used to develop semi-analytical fitting models for degradation.

Reference [10] presents a simple parameter based model for predicting battery lifetime under a uniform cycling scheme. For nonuniform cycling, a distribution of current rates is assumed. The lifetime model can be easily converted to a degradation model. It is used in the paper to develop a power control strategy for a hybrid battery/utra-capacitor storage system in electric vehicles. It is a suitable model when cycling parameter distributions can be assumed. However, it is unclear if this model will remain useful in optimization problems where the decisions change the profile of cycles.

Reference [11] develops another cycle based degradation model for the optimization of charging profiles in electric vehicles. The optimization uses time varying electricity costs and estimated degradation costs. It finds various charging optimal charging profiles based on the form of these costs.

Reference [12] develops a degradation model based directly on state of charge for use in an economic optimization of a hybrid battery/ photo-voltaic system. Though the functional form of state of charge degradation is complicated in this model, it is useful because many applications can use the battery's state of charge directly as a decision variable. The model's main disadvantage is that it does not have any direct consideration of depth of discharge. The optimization procedure took care of depth of discharge loss by putting upper and lower bounds on the state of charge.

A similar optimization problem was considered in [13]. In this paper, a semi-analytical degradation model, based on the properties found in [9], is developed. Through rainflow counting on real data, this paper finds a distribution of cycle parameters and uses this to find optimal charging profiles in hybrid battery/photo-voltaic systems. The model is also used to determine the best of three possible charging profiles for mobile phone longevity.

Other cycle parameter degradation models include reference [14], which optimizes a hybrid battery/HVAC system scheduling with battery degradation included, and reference [15] which considers battery degradation in an economic optimization of battery integration in a standalone microgrid.

This article has been accepted for publication in a future issue of this journal, but has not been fully edited. Content may change prior to final publication. Citation information: DOI 10.1109/TSG.2017.2695196, IEEE Transactions on Smart Grid

Some work has been done in coupling ancillary services with degradation. Most of these focus on battery control while providing ancillary services rather than on deciding how much ancillary service to provide at a given time. For example, reference [16] coupled degradation to a control strategy for peak shaving. In particular, reference [17] formulated frequency regulation as a nonlinear tracking problem and included a degradation model as a state variable which is to be driven to zero during the tracking. We believe these works to be applicable in conjunction with the work presented here by using the regulation decisions from our scheme with the control strategies of those.

Reference [18] is the closest work to this paper. It derives a simplified (though still nonlinear) degradation model that avoids rainflow counting and embeds it into an ancillary service optimization problem. The paper found good results and is a great exploration into coupling degradation considerations with ancilliary service scheduling. However, the results are found by optimizing over just one representative day and multiplying the daily profit by the lifetime (in days) that the representative day's operation would yield. The critical limitation to this approach is that it assumes lifetime can be accurately calculated from one day of battery operation. Realistic operation of a battery will vary day to day, and so a degradation model that considers the operations of each day is necessary.

III. External Degradation

A. Valuation Linear Program

Reference [6] introduced a linear program (LP) for valuating energy storage systems. The LP partitions the battery's available capacity at each hour $t = 1, 2, ..., \mathcal{T}$ into a set of profitable actions. These actions are discharging, d_t, providing regulation up services, r_t^u, and providing regulation down services, r_t^d. d_t is negative when the battery charges. r_t^u and r_t^d are strictly nonnegative. Each action has a corresponding revenue. These are the locational marginal price, LMP_t, which is the revenue from discharging $1MWh$ of energy, and $Reg_t^{u/d}$, the revenue from committing $1MWh$ of battery capacity to regulation services at hour t. A negative revenue, O_t, is included to incur small profit losses from battery use. It represents the cost of operation and maintenance, but its effect is small.

Only a fraction of the capacity committed to either regulation services will be used in real time operations. The amount used in regulation up is sold at the locational marginal price, and the amount used in regulation down is bought at this price. Denote these proportions as p_t^u and p_t^d for regulation up and down respectively. Then regulation up and down have an additional source of revenue through real time energy exchange given by $LMP_t p_t^{u/d} r_t^{u/d}$.

The decision variables of the LP are formed by appending a state variable, S_t, to the above actions. S_t represents the battery's State of Charge (SoC) at the beginning of hour t and follows simple update dynamics. We will place these decision variables in a vector $\mathbf{x}_t$ and contain the respective revenues in a matrix $\mathbf{A}_t$

$$\mathbf{x}_t = \begin{bmatrix} d_t & r_t^u & r_t^d & S_t \end{bmatrix}^T \tag{1}$$

$$\mathbf{A}_t = \begin{bmatrix} LMP_t & Reg_t^u & Reg_t^d & 0 \\ 0 & LMP_t \cdot p_t^u & -LMP_t \cdot p_t^d & 0 \\ 0 & -O_t \cdot p_t^u & -O_t \cdot p_t^d & 0 \end{bmatrix} \tag{2}$$

This ensures that the sum of entries of the vector $\mathbf{A}_t \mathbf{x}_t$ yeilds the total revenue at hour t.

The horizon of the LP is the estimated battery lifetime. We denote it as $\mathcal{T}$. It should be an overestimate of the battery's true lifetime. Decision variables beyond the true lifetime can be discarded later.

The LP is then given by objective function (3) and constraints (4 - 12).

$$\max_{\mathbf{x_t}} \quad \sum_{t=0}^{\mathcal{T}} \mathbf{1}^T \mathbf{A}_t \mathbf{x}_t \tag{3}$$

Subject to

$$\begin{aligned} S_{t+1} = S_t(1-\gamma) &- (d_t + p_t^u r_t^u - p_t^d r_t^d) \cdot (1\ hr.) \\ &- (|d_t| + p_t^u r_t^u + p_t^d r_t^d) \cdot (1\ hr.) \cdot \rho \end{aligned} \tag{4}$$

$$0 \ \leq S_t \ \leq \ E_{max} \tag{5}$$

$$(-d_t + r_t^d) \cdot (1\ hr.) \ \leq \ E_{max} - S_t \tag{6}$$

$$(d_t + r_t^u) \cdot (1\ hr.) \ \leq \ S_t \tag{7}$$

$$d_t + p_t^u r_t^u - p_t^d r_t^d \leq P_{max} \tag{8}$$

$$-d_t + p_t^d r_t^d - p_t^u r_t^u \leq P_{max} \tag{9}$$

$$d_t + r_t^u \leq P_{max} \tag{10}$$

$$-d_t + r_t^d \leq P_{max} \tag{11}$$

$$r_t^u, r_t^d \geq 0 \tag{12}$$

The first constraint is the update equation for the battery's state of charge. The constraint's first term is the battery's self-discharge which occurs with rate γ. The second term is the change in energy from the battery's actions, and the third term represents resistive losses that scale with total output power. The resistive losses, ρ, are derived from the battery's round-trip efficiency κ.

$$\rho = 1 - \sqrt{\kappa}$$

Constraints (5), (6), and (7) capture the fact that the battery's capacity must be partitioned. E_{max} is the battery's maximum state of charge. These constraints ensure that no physical constraint is violated even when all of the committed regulation capacity is used.

Finally, the battery's total output power is constrained by constraints (8), (9), (10), and (11). P_{max} is the battery's maximum power output.

Degradation is implemented by partitioning the LP into segments of T hours and optimizing each segment sequentially. The battery's degradation over each segment is calculated at the end of each iteration. From this calculation, a new value of E_{max} is fed into the next segment's constraints.

The algorithm runs over N iterations of the above such that $NT = \mathcal{T}$. We call this procedure *External Degradation* as the

This article has been accepted for publication in a future issue of this journal, but has not been fully edited. Content may change prior to final publication. Citation information: DOI 10.1109/TSG.2017.2695196, IEEE Transactions on Smart Grid

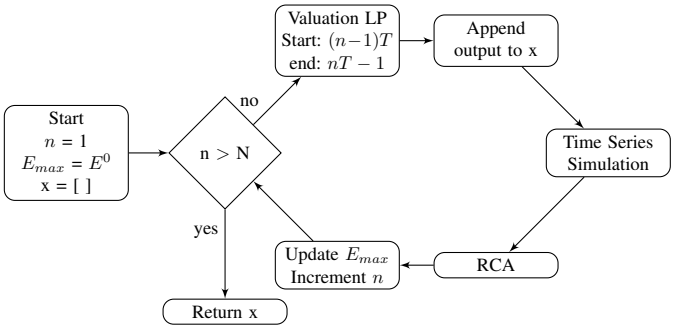

Fig. 1. External Degradation algorithm flowchart.

degradation calculation is external to the optimization. It is illustrated in Figure 1.

T determines a trade-off between optimality and degradation accuracy. Higher values of T will yield more optimal decision variables, but lower values of T (and thus more degradation updates) will lead to more accurate values of E_{max}. T does not need to be very small, however, because E_{max} changes rather slowly with time ($\approxeq 3\%$ per year). Furthermore, T does not need to be too large because the final outputs of the LP, as a function of T, converge when T exceeds 2 months. In this paper, T was chosen to represent yearly segments with an expected lifetime of 15 years ($N = 15, T = 8760$ hours).

In this optimization scheme and all optimization schemes to come, we considered a realization of prices that combines the methods of future price curve modeling in [6] with expert opinions and industry price models. The two data sets used (one for locational marginal prices and one for ancillary service prices) can be found at [19].

The External Degradation LP relies on long term forecasting of market prices. These prices are quite volatile in practice, however, so the results of the LP represent a clairvoyant upper bound on the actual value of a BESS.

B. Degradation Model

To calculate a segment's degradation, the semi-empirical model of [20] was implemented. The model is based on experimental data provided by ABB and EEH power systems laboratories. Its form is primarily based on the Arrhenius equation and the principle of cumulative degradation. This is similar to several of the models referenced in the literature review and so it is quite general. It is a parameter based model that is agnostic to battery type where different battery types will require different parameters. Its use is decomposed into the following three steps.

1) Regulation Signal and Intra-hour SoC Simulation: The SoC, as a function of time, must first be calculated. Its intra-hour behavior is determined by the regulation signal. When the r_t^u and r_t^d decision variables are nonzero, the battery is committed to provide regulation services throughout hour t. The battery is then required to adjust its output up to 900 times throughout the hour in response to regulation signals. This process can be simulated through the following intra-hour version of (4).

$$S_{t,k+1} = S_{t,k} + (r_t^d f_{t,k}^d - d_t - r_t^u f_{t,k}^u - \rho\,|d_t|)/900 \cdot (1\ hr.); \quad S_{t,0} = S_t \tag{13}$$

where t is the index of the hour being simulated (a constant), and k is an index representing the number of regulation ticks that have occurred since the start of hour t, i.e. $k = 1, 2, ...900$. f^u and f^d are the positive and negative parts of the regulation signal, f, respectively.

$$f_{t,k}^u = max\,(0, f_{t,k}) \qquad f_{t,k}^d = max\,(0, -f_{t,k}) \tag{14}$$

Terms involving the multiplication of ρ and $f^{(d/u)}$ in (13) have been ignored for being small. A year's worth (2015) of historical regulation signals from the PJM interconnection [21] were used.

2) Rainflow Counting: Once the SoC time series is known, it is fed into the Rainflow Counting Algorithm (RCA) [22]. The RCA is used to detect repetition in an aperiodic time series and compute a list of cycles, nonuniform in amplitude and duration, that are embedded within each other. Each cycle in this list is represented as an ordered set of parameter values. For battery degradation, the useful parameters are the Depth of Discharge (DoD), defined as the amplitude of a cycle normalized to the maximum battery capacity, the mean SoC, defined as the average of the cycle with time taken into account, and the current rate (CR), defined as the DoD divided by the cycle duration. Typically, the first step of the RCA reduces the input time series to a set of peak and valley values. This removes all knowledge of time, and so duration can not be calculated with this set up. To fix this, we have augmented the first step so that it keeps the intra-hour time indices at which the peaks and valleys occurred.

When referencing cycle values, SoC, DoD, and CR will all refer to values that are normalized by the current E_{max}, and thus belong to the interval $[0, 1]$. However, we will occasionally reference the SoC time series. Values of SoC, as evaluations of this time series, will not be normalized.

3) Capacity Calculation: The new maximum capacity is obtained from the outputs of the RCA as follows. First, for each cycle (indexed by i), the following three semi-empirical functions are calculated

$$f_{DoD}(DoD_i) = (k_{DoD,1} DoD_i^{-k_{DoD,2}} - k_{DoD,3})^{-1} \tag{15}$$

$$f_{SoC}(SoC_i) = e^{k_{SoC}(SoC_i - SoC_{ref})} \tag{16}$$

$$f_{CR}(CR_i) = e^{k_{CR}(CR_i - CR_{ref})} \tag{17}$$

Where DoD_i, SoC_i, and CR_i are the DoD, SoC and CR of the i^{th} cycle. The forms of these functions are derived from theoretical considerations. Parameter values for Lithium-Ion (Li-Ion) batteries were found experimentally in [20]. Table I repeats these values for convenience.

This article has been accepted for publication in a future issue of this journal, but has not been fully edited. Content may change prior to final publication. Citation information: DOI 10.1109/TSG.2017.2695196, IEEE Transactions on Smart Grid

TABLE I
DEGRADATION FUNCTION PARAMETERS FOR A LI-ION BATTERY.

Function Parameters		
Stressor	Parameter	Value
DoD	$k_{DoD,1}$	8.95×10^4
	$k_{DoD,2}$	4.86×10^{-1}
	$k_{DoD,3}$	7.28×10^4
SoC	k_{SoC}	1.04
	SoC_{ref}	0.50
CR	k_{CR}	2.63×10^{-1}
	CR_{ref}	1.00
Time	k_t	$1.49 \times 10^{-6} \frac{1}{hr}$
r_1		5.75×10^{-2}
r_2		121

A degradation rate deg_n is then calculated from these functions according to (18).

$$deg_n = \sum_{i=1}^{L_n} f_{DoD}(DoD_i) f_{SoC}(SoC_i) f_{CR}(CR_i) + k_t T \tag{18}$$

where L_n is the number of cycles that occurred during step n and k_t is the rate at which the battery ages independently from operation. We will call deg_n the *degradation function*, viewing it as a function of cycles and time.

Finally, the new capacity is calculated from the following double exponential model.

$$E_{max}^{(n+1)} = r_1 e^{-r_2 \sum_{\eta=1}^{n} deg_\eta} + (1 - r_1) e^{\sum_{\eta=1}^{n} deg_\eta} \tag{19}$$

The first exponential represents a quick degradation from the build up of the Solid Electrolyte Interphase (SEI) layer. The second represents a slower degradation from ion loss. Values for r_1 and r_2 are provided in Table I.

The effect of power fade was not considered in this paper. Power fade occurs as a build up of internal resistance in the battery which reduces κ and P_{max}. However, its primary stressor (aside from time) becomes important only when the battery's SoC is held near its boundaries for extended periods of time [23]. As we will see in section IV, the optimized SoC time series is rarely near either boundary, and so this stressor can be ignored.

P_{max} is changed in the external degradation setup only when $E_{max}/(1\ hr.)$ degrades below the nominal P_{max}. In this case, P_{max} is set to E_{max} for the remaining simulations.

IV. OUTPUT PROPERTIES

A. Macro Cycles and Micro Cycles

Figure 2 shows a day's worth of the SoC time series, found through the external degradation procedure, for a battery with energy rating $5.8MWh$ and power rating $2.53MW$. Observed is a clear separation in magnitude between the high frequency cycles and the low frequency ones. It is useful to think of

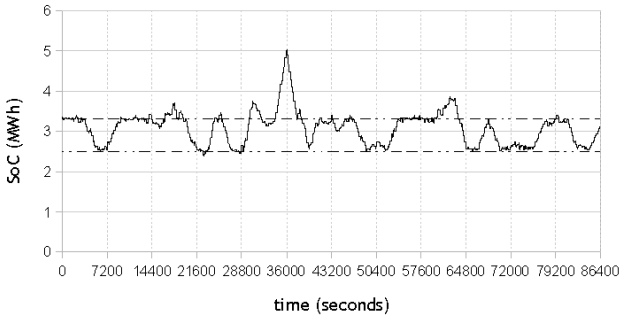

Fig. 2. Time series data of the SoC over a sample 24 hour window.

the state of charge time series as the sum of a low frequency component and a high frequency perturbation. We will further consider the state of charge over the interval $[t, t+1]$ as a continuous time function $\psi_t(\tau)$, $\tau \in [0, 1](hrs.)$. This should be a decent approximation because the update time for the state of charge time series (4 sec) is much smaller than time scale required for significant degradation ($\approxeq$ 1 year). We will call ψ the state of charge *profile* to distinguish it from the state of charge time series.

The decomposition of ψ will be as follows. Denoting the low frequency component as ψ_M and the high frequency component as ψ_m, we have

$$\psi_t(\tau) = \psi_{t,M}(\tau) + \psi_{t,m}(\tau) \tag{20}$$

where

$$\psi_{t,M}(\tau) = (S_t - S_{t+1}) \cdot \tau \tag{21}$$

$$\psi_{t,m}(\tau) = \psi_t(\tau) - \psi_{t,M}(\tau) \tag{22}$$

That is, ψ_M is obtained from linear interpolation of the S decision variables and ψ_m is obtained by removing the low frequency component from ψ. We will consider these continuous functions as valid inputs to the RCA (where, realistically, we run it on the un-approximated time series). We will denote the high frequency cycles as micro cycles and the low frequency ones as macro cycles.

B. Bounding Region and Switching Behavior

Figure 2 illustrates a second important property: the SoC is attracted to the values 2.5 KWh and 3.3 KWh. Furthermore, it frequently abandons its current value for the other. Note that these attraction values are $P_{max} \cdot (1\ hr.)$ and $E_{max} - P_{max} \cdot (1\ hr.)$ respectively.

This is no coincidence. The valuation LP can be viewed as an optimization over one state changing variable (charging/discharging) that can be either costly or profitable, and one non-state changing variable (regulation up and down simultaneously) that is always profitable. Intuitively, we would like for the non-state changing variable to be maximized as often as possible. The following proposition establishes the existence of a SoC region in which this is possible.

This article has been accepted for publication in a future issue of this journal, but has not been fully edited. Content may change prior to final publication. Citation information: DOI 10.1109/TSG.2017.2695196, IEEE Transactions on Smart Grid

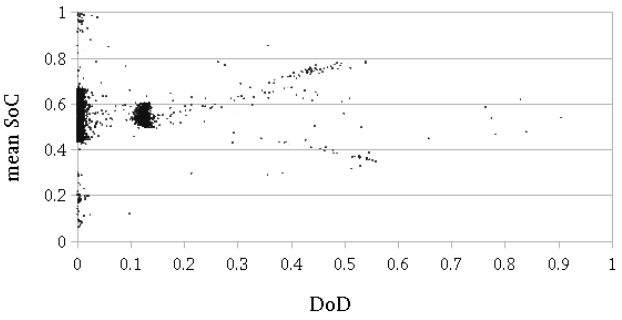

Fig. 3. Scatterplot of mean normalized SoC vs. normalized DoD.

Proposition 1. *The maximum value of* $r_t^u + r_t^d$ *is* $E_{max}/(2\ hrs.) + P_{max}$. *This maximum is achievable iff.* $S_t \in \mathcal{I} = [u, v]$ *where* u *and* v *are the minimum and maximum of* $\{P_{max} \cdot (1\ hr.), E_{max} - P_{max} \cdot (1\ hr.)\}$ *respectively.*

This is proved in the Appendix. We name the region $\mathcal{I}$ the SoC *Bounding Region*. The proposition and the above logic help to explain the observation that the SoC profile tends to stay within this region, but it does not explain the behavior of repeatedly switching from bound to bound.

To understand the switching behavior, we note that the profit from discharging will occasionally dominate over the profit from regulation services. When this happens, we will want to discharge as much as possible. However, we will want the SoC to remain in $\mathcal{I}$. It makes sense, then, to discharge from the upper bound of $\mathcal{I}$ to the lower bound. Then sometime before this discharge, the SoC will need to be brought to the upper bound of $\mathcal{I}$, and we will want to do this when charging is cheapest. It follows that this SoC raise will occur in one step (at the time when charging is cheapest). For similar reasons, the subsequent discharge will also occur in one step.

It is never the case, in the scope of this paper, that the length of $\mathcal{I}$ is too large to charge or discharge in a single step. If this were the case, we would have $|2P_{max} \cdot (1\ hr) - E_{max}| > P_{max} \cdot (1\ hr)$. But this requires that $E_{max} < P_{max} \cdot (1\ hr.)$. This is only the case in special situations which are not considered here.

Define R as half the length of $\mathcal{I}$ normalized by E_{max}.

$$R \triangleq \left| \frac{1}{2} - \frac{P_{max} \cdot (1\ hr.)}{E_{max}} \right| \tag{23}$$

Then $\mathcal{I} = [E_{max} \cdot (\frac{1}{2} - R), E_{max} \cdot (\frac{1}{2} + R)]$

C. Bimodality and Symmetry

Since the SoC time series frequently jumps in value from $E_{max} \cdot (\frac{1}{2} - R)$ to $E_{max} \cdot (\frac{1}{2} + R)$ and back, we will have a build up of macro cycles with DoD near $2R$. The micro cycles and most of the remaining macro cycles will have DoDs much lower than this. Thus, with respect to DoD, we obtain a bimodal distribution.

The cycles in either of these peaks are equally likely to occur above or below $SoC = \frac{1}{2}E_{max}$. Thus we have symmetry in that, for any range of DoD values, the number of cycles with mean SoC above this line will be nearly equal to the number of cycles with mean SoC below it.

Both of these properties are illustrated in Figure 3 which plots the SoC (normalized to E_{max}) against the DoD (also normalized) for a year's worth of cycles. The figure displays a distinct gap in the DoD direction and rough symmetry about the $SoC = \frac{1}{2}$.

D. Scope

These output properties depend only on the form of the external degradation LP and the general relative magnitudes of prices for each service. They do not depend on any particular instance of prices in the objective function. However, this LP does assume perfect forecasting of prices, and so it is reasonable to question the retainment of these properties in more realistic scenarios, e.g. stochastic optimization. A greedy algorithm, for example, could see a large discharge profit and go well below $\mathcal{I}$. Thus one does need to be careful to ensure that their optimization strategy complies with the above heuristics (keeping the SoC in $\mathcal{I}$, charging and discharging the entire boundary in one step) before invoking these properties.

More optimistically, these properties can be used to guide local decision making. The global behavior of the clairvoyant LP is explained by *local* heuristics. It stands to reason that local decisions based on these heuristics will approximate the decisions made by the clairvoyant strategy. We suspect that a stochastic optimization problem on just energy arbitrage with loss functions included to punish the SoC for leaving $\mathcal{I}$ could yield profits close to those of the clairvoyant bound (assuming maximum regulation in both directions is always provided). Under such a scheme, the above properties can be invoked without guilt.

Furthermore, if the relative magnitudes of prices are consistently different from those used here, the properties could break down. For example, if regulation services consistently have negligible revenue compared to arbitrage, then the LP will have no reason to keep the SoC inside $\mathcal{I}$. We believe that the price path used does, at the least, capture these magnitudes realistically, so, this problem should not last for long if it does occur.

V. Linearization

We will now begin to describe the process of simplifying the degradation model that

1) depends on the decision variables instead of the rainflow counted cycles.
2) is linear.

We will first show that the current rate component, f_{CR}, and state of charge component f_{SoC} can be reasonably approximated as constants. The particular values of every constant that follows depends on the battery type, but all can be derived from the same process. We list the values derived for Li-ion batteries in this paper.

This article has been accepted for publication in a future issue of this journal, but has not been fully edited. Content may change prior to final publication. Citation information: DOI 10.1109/TSG.2017.2695196, IEEE Transactions on Smart Grid

A. Current Rate Component

Most ($\approxeq 99\%$) of the realized cycles have current rate on the order of 0.1 or smaller. This is because micro cycles have small DoD, and macro cycles have long time scales. The current rates of the remaining cycles are too few and not large enough ($\approxeq 0.25$) to significantly influence the degradation of the battery. Since the component of degradation due to current rate varies slowly for these small rates, we take f_{CR} to be the constant $J_{CR} = 0.785$ ($CR \approxeq 0.08$).

B. Lebesgue Integral Reformulation

For the remaining subsections, we will rewrite the cycle degradation component of (18) as a Lebesgue integral over a constructed measure space.

Let C_n be the set of all cycles returned from the RCA after iteration n. $\forall c \in C_n$, denote the depth of discharge and mean state of charge of c as $DoD(c)$ and $SoC(c)$ respectively. Let X and Y be unit intervals and let $\mathcal{B}_X$ and $\mathcal{B}_Y$ be the Borel σ-algebras on X and Y. Let ν be the push-forward measure of the counting measure on C_n through the function

$$c \mapsto \begin{bmatrix} DoD(c) \\ SoC(c) \end{bmatrix}$$

Then $(X \times Y, \mathcal{B}_X \otimes \mathcal{B}_Y, \nu)$ is a σ-finite measure space because $\nu(X \times Y) < \infty$. Intuitively, ν counts the number of dots in a given subset of Figure 3.

The cycle component of the degradation function can then be written as the following Lebesgue integral.

$$f = J_{CR} \int_{X \times Y} f_{SoC}\ f_{DoD}\ d\nu \tag{24}$$

This transfers the sum over each cycle in (18) into a sum over possible output values $(f_{CR} \cdot f_{SoC} \cdot f_{DoD})$ times the number of cycles that yield that value $(d\nu)$.

C. State of Charge Component

The symmetry discussed in section IV-C reduces the SoC component of the degradation function to a constant (approximately). To see this, let $\pi_x : X \times Y \to X$ be a projection to the x-axis. Let μ be the pushforward measure $\mu = \nu \circ \pi^{-1}$. By the disintegration theorem [24], there exists a family of conditional measures $\{\nu_x\}_{x \in X}$ such that $\nu_x(\{x\} \times Y) = 1$ $\forall x \in X$ and (24) can be rewritten as the following iterated integral.

$$f = J_{CR} \int_X f_{DoD} \left(\int_{\{x\} \times Y} f_{SoC}\ d\nu_x \right) d\mu \tag{25}$$

Now split the y-axis at $\frac{1}{2}$ and denote the lower and upper halves as Y^- and Y^+ respectively. Let h reflect $y \in Y^-$ across the $y = \frac{1}{2}$ axis, i.e. $h(y) = 1 - y$. Symmetry implies that the pushforward of ν_x under h is just ν_x, so the inner integral can be written as follows.

$$\begin{aligned} \int_{\{x\} \times Y} f_{SoC}\ d\nu_x &= \int_{\{x\} \times Y^-} f_{SoC}\ d\nu_x + \int_{\{x\} \times Y^+} f_{SoC}\ d\nu_x \\ &= \int_{\{x\} \times Y^+} \left(f_{SoC} \circ h + f_{SoC}\right) d\nu_x \end{aligned} \tag{26}$$

But (relying on the chosen value of $SoC_{ref} = \frac{1}{2}$)

$$\begin{aligned} \left(f_{SoC} \circ h + f_{SoC}\right)(y) &= e^{k_{SoC}(1-y-\frac{1}{2})} + e^{k_{SoC}(y-\frac{1}{2})} \\ &= 2cosh\left(k_{SoC}\left(y - \frac{1}{2}\right)\right) \end{aligned}$$

which varies slowly for $y \in Y^+$. We can therefore approximate it as a constant. We chose to take its average over Y^+, $J_{SoC} = 1.0422$, as the constant in question. Equation (26) then becomes $2J_{SoC} \cdot \nu(Y^+)$. Symmetry implies that Y^+ has ν_x-measure $\frac{1}{2}$ $\forall x \in X$, so this is just J_{SoC}.

The degradation function now takes the form

$$f = J_{CR} \cdot J_{SoC} \int_X f_{DoD} d\mu \tag{27}$$

(27) is a 1-dimensional analog of (24) which relies on DoD alone.

D. Depth of Discharge Component

All that remains to simplify is the DoD component of the degradation function.

1) Cycle Splitting: The integrand in (27) can be split by cycle type. Explicitly, we create two new measures for $A \in \mathcal{B}_X$, one that counts the number of *micro* cycles with DoD in A and one that counts the number of *macro* cycles with DoD in A. We call these μ_m and μ_M respectively. Both are dominated by μ because a subset cannot contain micro or macro cycles if it does not contain any cycles. Thus there exist Radon-Nikodym derivatives g_m and g_M such that

$$\mu_m(A) = \int_A g_m d\mu \tag{28}$$

$$\mu_M(A) = \int_A g_M d\mu \tag{29}$$

clearly $\mu(A) = \mu_m(A) + \mu_M(A)\ \forall\ A \in \mathcal{B}_X$ because the number of cycles in A is equal to the number of mirco cycles in A plus the number of macro cycles in A. Then (27) becomes

$$f = J_{CR} J_{SoC} \cdot \left(\int_X f_{DoD}\ d\mu_m + \int_X f_{DoD}\ d\mu_M \right) \tag{30}$$

All micro cycles are contained in the first peak of the bimodal DoD distribution. As illustrated in figure 4, we can linearize f_{DoD} in the small DoD region quite well.

On the other hand, macro cycles can belong to either peak. Since the slope of f_{DoD} is different at both of these peaks, it may be thought that no one line can approximate the degradation from a set of cycles belonging to both. However, there are so few cycles in between these peaks that a line from zero to the second peak will actually work as a decent approximation. This, of course, requires that we know where the second peak is; luckily, we already know that this is $2R$. We can thus fully linearize (30) as

$$f = J_{CR} \cdot J_{SoC} \cdot \left(a_1 \int_X x\ d\mu_m + a_2 \int_X x\ d\mu_M \right) \tag{31}$$

This article has been accepted for publication in a future issue of this journal, but has not been fully edited. Content may change prior to final publication. Citation information: DOI 10.1109/TSG.2017.2695196, IEEE Transactions on Smart Grid

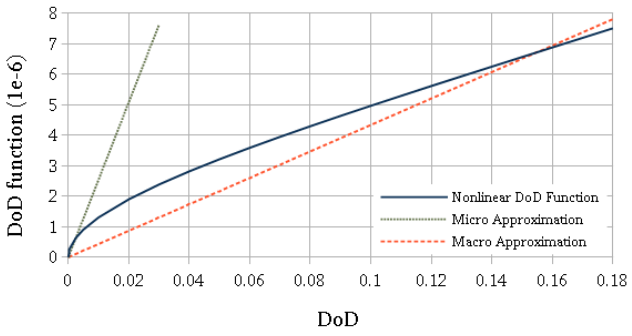

Fig. 4. f_{DoD} and corresponding linearizations.

2) Quadratic Functional Expansion: Rewrite (31) as

$$f = J_{CR}J_{SoC}\Big(\int_X x\,(a_1 g_m + a_2 g_M)\;\; d\mu\Big) \tag{32}$$

and define $g = a_1 g_m + a_2 g_M$. This is the Raydon-Nikodym derivative of a new measure that counts a scaled version of the macro cycles and adds to it a scaled version of the micro cycles. If a_1 and a_2 are of the same magnitude, then this new measure can be interpreted as an approximation to the measure that counts the number of cycles in X of an augmented state of charge profile $\tilde{\psi}_t(\tau) = a_1\psi_{t,m}(\tau) + a_2\psi_{t,M}(\tau)$.

Under this interpretation, the integrand in (32) is equivalent to the total depth of discharge traversed by $\tilde{\psi}_t$. This is equal to half of the total absolute change in $\tilde{\psi}_t$. We can thus model the integral in (32) as the nonlinear functional

$$\phi(\tilde{\psi}_t) = \frac{1}{2}\int_0^1 \left|\frac{d\tilde{\psi}_t(\tau)}{d\tau}\right| d\tau. \tag{33}$$

We will drop the subscript t on all ψ and $\tilde{\psi}$ symbols. For what remains of this subsection, all calculations are considered within hour t.

Considering $a_1\psi_m$ as a small perturbation on $a_2\psi_M$, we can approximate (33) by the functional Taylor series [25, Appendix A]

$$\begin{aligned}\phi(\tilde{\psi}) \approx \phi(a_2\psi_M) + a_1\frac{d\phi(a_2\psi_M + \varepsilon\psi_m)}{d\varepsilon}|_{\varepsilon=0} \\ + \frac{1}{2}{a_1}^2\frac{d^2\phi(a_2\psi_M + \varepsilon\psi_m)}{d\varepsilon^2}|_{\varepsilon=0}\end{aligned} \tag{34}$$

The zero order term is just

$$\begin{aligned}\frac{1}{2}|a_2\psi'_M| = \frac{a_2}{2}\big|(1-\rho)(p_t^d r_t^d) \\ -(1+\rho)(p_t^u r_t^u) - d_t - \rho|d_t|\big|\end{aligned} \tag{35}$$

as no term in ψ'_M has intra-hour time dependence.

To obtain the first order term, we must differentiate the non-differentiable integrand of (33). Thus we approximate this integrand with the differentiable function $((\frac{d\psi}{dt})^2 + u^2)^{\frac{1}{2}}$ and consider what happens as $u \to 0$. The first order term is then

$$\frac{a_1 a_2 \psi'_M}{2(a_2^2\psi_M'^2 + u^2)^{\frac{1}{2}}}\int_0^1 \psi'_m dt \tag{36}$$

This term will vanish because within the hour,

$$\psi'_m(t) = r_t^u(f_t^u - p_t^u) + r_t^d(p_t^d - f_t^d) \tag{37}$$

(where the loss factor ρ has been ignored because all terms involving it in ψ'_m are small) and $\int_0^1 f_t^{u/d}dt = p_t^{u/d}$.

The second order term is given by

$$\frac{a_1^2 u^2}{4(a_2^2\psi_M'^2 + u^2)^{\frac{3}{2}}}\int_0^1 \psi_m'^2 dt \tag{38}$$

But

$$\begin{aligned}\int_0^1 \psi_M'^2 dt = \mathbb{V}ar\left[r_t^u f^u(t)\right] + \mathbb{V}ar\left[r_t^d f^d(t)\right] \\ -\mathbb{E}\left[2r_t^u r_t^d \tilde{f}^u(t)\tilde{f}^d(t)\right]\end{aligned} \tag{39}$$

where $\tilde{f}^u(t) = (f^u(t) - p_t^u)$, $\tilde{f}^d(t) = (f^d(t) - p_t^d)$, and the statistics are taken as time integrations over the hour under consideration. We will write $\mathbb{V}ar\left[f^u(t)\right]$ as $\sigma_{t,u}^2$ and $\mathbb{V}ar\left[f^d(t)\right]$ as $\sigma_{t,d}^2$. These can be calculated (or estimated if the signal is not known [26]) before simulation.

Since f^u and f^d are never simultaneously nonzero and $\mathbb{E}[f^{u/d}] = p_t^{u/d}$, the expectation term can be calculated as $-2r_t^u r_t^d p_t^u p_t^d$. The variance terms can be written as

$$(r_t^u + r_t^d)(r_t^u\sigma_{t,u}^2 + r_t^d\sigma_{t,d}^2) - r_t^u r_t^d(\sigma_{t,u}^2 + \sigma_{t,d}^2)$$

Finally, as $u \to 0$,

$$\frac{u^2}{(a_2^2\psi_M'^2 + u^2)^{\frac{3}{2}}} \to \frac{2}{a_2}\delta(\psi'_M)$$

where $\delta(\cdot)$ is the dirac-delta impulse function. Thus the second order term is nonzero only during hours in which $\psi'_M = 0$. This implies that, to the second order, there is complete separation between the macro and micro cycles in terms of degradation.

The second order term is then

$$\begin{aligned}\delta(\psi'_M)\frac{a_1^2}{2a_2}\Big((r_t^u + r_t^d)(r_t^u\sigma_{t,u}^2 + r_t^d\sigma_{t,d}^2) \\ -r_t^u r_t^d(\sigma_{t,u}^2 + \sigma_{t,d}^2 + 2p_t^u p_t^d)\Big)\end{aligned} \tag{40}$$

3) Remaining Nonlinearities: For a fully linear model, we must find a way to remove the absolute value and delta functions from these formulas. We must also remove the quadratic regulation terms. We choose to do this statistically, i.e. by considering the effects of summing each hour's degradation component over the time interval simulated (e.g. one year).

Let U_z be the set of hours in which $\psi'_M = 0$. Let H be the set of all hours simulated in a given block and $p_z = \frac{|U_z|}{|H|}$. Unfortunately, this must be known before the simulation. However, if it is guessed and updated, it only takes about two iterations for it to converge.

For hours in U_z, there is no change in state of charge to compute. In $H - U_z$, we assume the state of charge increases and decreases with equal probability and assume further that d_t is positive when it decreases and negative otherwise. The absolute value function in (35) can then be approximated as $\frac{1}{2}(1-p_z)|d_t|$ and since d_t appears directly in the objective

This article has been accepted for publication in a future issue of this journal, but has not been fully edited. Content may change prior to final publication. Citation information: DOI 10.1109/TSG.2017.2695196, IEEE Transactions on Smart Grid

function, it can be split into two variables, d'_t and c'_t (for discharge and charge) such that $d_t = d'_t - c'_t$ and $|d_t| = d'_t + c'_t$.

We evaluate the second order term similarly by replacing $\delta(\psi'_M)$ with it's expectation over several possible ψ'_M (as many will occur over the course of a year), p_z.

Finally, the constraints of the LP enforce that $(r_t^u + r_t^d) \leq 2P_{max}$ in $\mathcal{I}$. In fact, maximizing this term is the reason that the SoC time series stays in this region in the first place. Thus we replace the sum with this bound entirely. We also replace the product $r_t^d r_t^u$ with $\frac{1}{2}P_{max}(r_t^u + r_t^d)$ by splitting the term into $\frac{1}{2}(r_t^u r_t^d + r_t^u r_t^d)$ and setting $r_t^u = P_{max}$ in the first term and $r_t^d = P_{max}$ in the second. We do not further approximate this sum as $2P_{max}$ because it is already linear.

The degradation constants for each decision variable are thus derived. We summarize the simplified model in (41 - 44)

$$\mathbf{b} = \begin{bmatrix} \frac{a_2}{4}(1-p_z) \\ \frac{a_2}{4}(1-p_z) \\ \frac{a_1^2}{2a_2}p_z P_{max}(1.5\sigma_{t,u}^2 - 0.5\sigma_{t,d}^2 - p_t^u p_t^d) \\ \frac{a_1^2}{2a_2}p_z P_{max}(1.5\sigma_{t,d}^2 - 0.5\sigma_{t,u}^2 - p_t^u p_t^d) \\ 0 \end{bmatrix} \tag{41}$$

$$X_t = \mathbf{b}^T \begin{bmatrix} c'_t \\ d'_t \\ r_t^u \\ r_t^d \\ S_t \end{bmatrix} \tag{42}$$

$$deg_n = \sum_{t=0}^{T} X_t + k_t \cdot T \tag{43}$$

$$E_{max}^{(n+1)} = r_1 e^{-r_2 \sum_{\eta=1}^{n} deg_\eta} + (1-r_1)e^{\sum_{\eta=1}^{n} deg_\eta} \tag{44}$$

where $a_1 = \frac{2R}{f_{DoD}(2R)}$, $a_2 = 1 \times 10^{-4}$, and k is a tuning parameter defined in the next section.

The final two calculations remain external to the optimization problem. However, the re-simulation step and the RCA algorithm are eliminated from the calculation. Most importantly, however, is that this degradation is explicitly a function on the decision variables of the LP, and can be incorporated *internal* to the optimization.

4) Caveats: The SoC time series output will never have exactly the ideal properties of section IV. Thus we use the tuning parameter k to mitigate this problem. k will almost always be near unity, and can be viewed as a non-ideality factor for the SoC profile. Tuning k does not take much effort. In our results, k was tuned to obtain small error on the first year and then the found value was used for every year after that.

Furthermore, the model is underpinned by the bi-modality of the DoD distribution. This bi-modality in turn depends on the R-gap. As the R-gap becomes small, the second peak approaches the first and a single mode distribution is obtained. Thus, when R is small (e.g. $R < 0.1$), a_1 should be set to $\frac{0.1}{f_{DoD}(0.1)}$ by default. Also, U_z should be more inclusive as the gap decreases because ψ'_M, when nonzero, is almost always extremely small (as the jumps become small), so micro cycles dominate these hours despite technically having nonzero ψ'_M. Thus, for years with $2R \leq 0.1$, we include hours into U_z if $\psi'_M \leq 1 \times 10^{-1}$ whereas we use the criterion $\psi'_M \leq 1 \times 10^{-12}$ for years that do not have this property. Realistically, this precaution will only be necessary for a few initial years because the nominal P_{max} is typically less than $\frac{1}{2}E_{max}/(1\ hr.)$.

Finally, when the R-gap is large, it becomes easier for the SoC time series to stay within the stable gap even when charging and discharging. This means that the optimization will discharge even when the profit of doing so only dominates by a small amount. Thus we expect to have more cycles within the R-gap as it gets larger. However, when discharging profit dominates regulation, it will still discharge by at least the smallest gap where a bimodal distribution was observed. It follows that there will still be distance between the micro cycles and macro cycles. Thus $a_2 = \frac{0.15}{f_{DoD}(0.15)}$ was used for years when $2R > 0.15$.

E. Internal Degradation

To test this model, a linear term is added to the objective function, (3), to punish high degradation. This leads to a modified version of the original linear program which we will call *Internal Degredation* to contrast it with the external procedure.

First, because we have split the discharge variable into its positive and negative parts (d'_t discharging and c'_t for charging), we need to modify the decision vector $\mathbf{x}_t$ and the revenue matrix $\mathbf{A}_t$.

$$\mathbf{x}'_t = \begin{bmatrix} c'_t & d'_t & r_t^u & r_t^d & S_t \end{bmatrix}^T \tag{45}$$

$$\mathbf{A}'_t = \begin{bmatrix} -LMP_t & LMP_t & LMP_t \cdot p_t^u & -LMP_t \cdot p_t^d & 0 \\ 0 & 0 & Reg_t^u & Reg_t^d & 0 \\ 0 & 0 & -O_t \cdot p_t^u & -O_t \cdot p_t^d & 0 \end{bmatrix} \tag{46}$$

The optimization problem then takes the form.

$$\max_{\mathbf{x}'_t} \sum_{t=0}^{\mathcal{T}} (\mathbf{1}^T \mathbf{A}'_t \mathbf{x}'_t + M_t^{deg} X_t) \tag{47}$$

Subject to

$$S_{t+1} = S_t(1-\gamma) - (d'_t - c'_t + p_t^u r_t^u - p_t^d r_t^d) \cdot (1\ hr.) - (d'_t + c'_t + p_t^u r_t^u + p_t^d r_t^d) \cdot (1\ hr.)\rho \tag{48}$$

$$0 \leq S_t \leq E_{max} \tag{49}$$

$$(c'_t + r_t^d) \cdot (1\ hr.) \leq E_{max} - S_t \tag{50}$$

$$(d'_t + r_t^u) \cdot (1\ hr.) \leq S_t \tag{51}$$

$$d'_t + p_t^u r_t^u - p_t^d r_t^d \leq P_{max} \tag{52}$$

$$c'_t + p_t^d r_t^d - p_t^u r_t^u \leq P_{max} \tag{53}$$

$$d'_t + r_t^u \leq P_{max} \tag{54}$$

$$c'_t + r_t^d \leq P_{max} \tag{55}$$

$$X_t = \mathbf{b}^T \mathbf{x}'_t \tag{56}$$

$$c'_t, d'_t, r_t^u, r_t^d \geq 0 \tag{57}$$

The optimization is still split into N iterations of horizon T. At the end of each iteration, (43) and (44) are calculated and the new E_{max} is fed into the next iteration.

This article has been accepted for publication in a future issue of this journal, but has not been fully edited. Content may change prior to final publication. Citation information: DOI 10.1109/TSG.2017.2695196, IEEE Transactions on Smart Grid

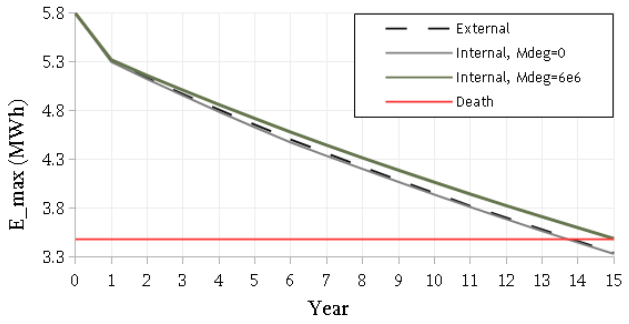

Fig. 5. E_{max} at the beginning of each year for three optimization schemes.

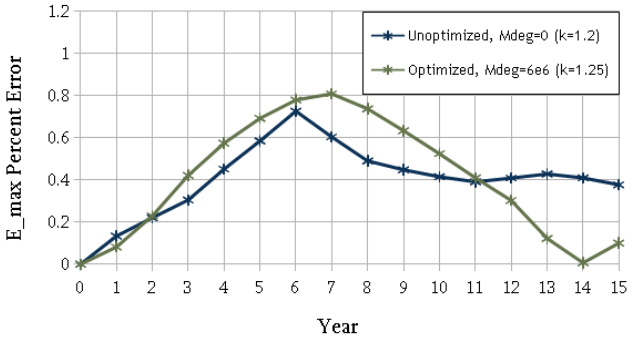

Fig. 6. Cumulative percent error in E_{max} after each year.

M_t^{deg} introduces a new trade off. If M_t^{deg} is too large, the LP will sacrifice far too much profit in return for extended battery lifetime. Even further, it will disturb the properties used to derive the linear model. Then the term $M_t^{deg} X_t$ may hurt profits without improving lifetime. If M_t^{deg} is too small, however, then the results of the new optimization scheme will reduce to that of the external degradation scheme. We name this procedure *Internal Degredation* to contrast it with the external procedure.

Since a cycle's degradation is on the order of 10^{-6}, and the remaining multipliers in the objective function are on the order of 1 dollar, we should let M_t^{deg} be on the order of 10^6. Several values of M_t^{deg} were tested. The results of these will be presented in the next section.

VI. Results

The validity of three claims will be shown in this section. The first claim is that the simplification of the degradation function is a good approximation of the actual degradation process. The second is that realistic degradation needs to be considered when valuing a battery energy storage system, and the final claim is that a significant portion of the value lost from the degradation processes can be recovered by using the above internal degradation formulation.

The battery and economic parameters used in the following simulations are shown in Table II.

TABLE II
Battery size and economic parameters.

Sizing and Economics			
Parameter	Value	Parameter	Value
E_{max}	$5.8MWh$	P_{max}	$2.53MW$
κ	88%	γ	$1.65\%/mo.$
Energy Investment	$\$614/kWh$	Power Investment	$\$551/kW$
Auxiliary Load	0.875%	Discount Rate	6%

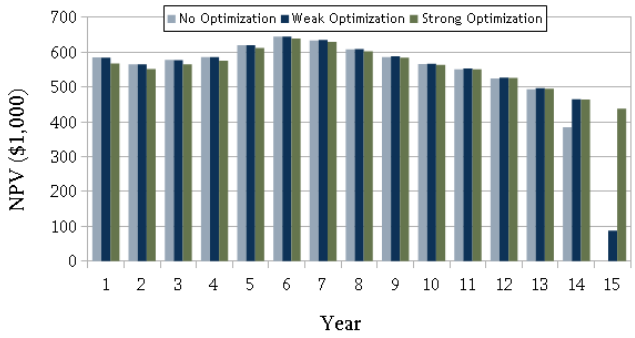

Fig. 7. Net Present Value (NPV) of each year.

A. Linearization Performance

Figure 5 shows three plots of E_{max} vs. year number. The lower two of these curves illustrate a direct comparison between the linearized degradation model (estimated) and the nonlinear, non-closed form degradation model (external) when both are used in the original LP with the same path of prices (or equivalently, when $M_t^{deg} = 0$). On the whole, the curve from the approximated model is lower than that of the nonlinear model. However, the curves are close. Thus the linear model well approximates the more complex one in this case.

Testing that this approximation performs well even when $M_t^{deg} \neq 0$ is critical. To test this, Internal Degradation was run with $M_t^{deg} = 6e6$ and a list of yearly E_{max} values was returned. A posteriori verification of the linearized model was then formed by combining using the optimization scheme of Internal Degradation (with $M_t^{deg} = 6e6$) but with degradation calculated from the nonlinear model. This verification also returned a list of yearly E_{max} values. The percent differences in the returned E_{max} values between the Internal Degradation scheme and the posteriori verification are plotted in Figure 6 (optimized, $M^{deg} = 6e6$). Figure 6 also plots the percent differences in E_{max} for the unoptimized ($M^{deg} = 0$) case. The error in the optimized case is not much worse than that of the unoptimized. However, in the latter case, k was raised slightly. The necessity of raising k implies that the LP properties were less ideal when $M^{deg} \neq 0$. In any case, all errors are bounded by 1%.

This article has been accepted for publication in a future issue of this journal, but has not been fully edited. Content may change prior to final publication. Citation information: DOI 10.1109/TSG.2017.2695196, IEEE Transactions on Smart Grid

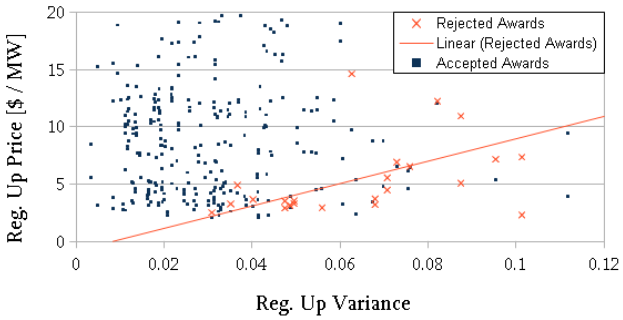

Fig. 8. Regulation Up signal variance vs. price. The trend line is $y = 97.86x - 0.81$.

B. Value Loss from Degradation

In a test case, External Degradation was modified to exclude cycle degradation. That is, (18) was changed to

$$deg_n = k_t T \tag{58}$$

The results of this were compared to an unmodified External Degradation procedure. In the test case, a BESS value of $\$1,700,000$ is obtained. In the latter, this value drops to $\$1,205,000$. Thus $\$495,000$ of value is lost to cycle degradation, a 29.1% loss. Cycle degradation represents a considerable loss to BESS value and needs to be considered.

C. Value Recovery

The higher E_{max} curve of Figure 5 is found from Internal Degradation with $M_t^{deg} = 6e6$. Critically, this curve crosses the $E_{max} = 3.48$ (60% nominal) line a whole year later than the lower two curves which represent External Degradation. Taking this E_{max} line as the death of the battery, we see that the battery optimized with Internal Degradation provides an additional year of value over the battery optimized with External Degradation.

This is illustrated in Figure 7. The two he two furthest right bars of this figure (at each year) represent Internal Degradation. The rightmost bar is obtained by using $M^{deg} = 6e6$, and the middle bar is obtained with $M^{deg} = 1e6$. The leftmost bar represents External Degradation. The initial investment is the same in all three cases ($\$6,730,000$, based on battery size). It is observed that Internal Degradation under-performs slightly in the earlier years, but by doing so it gains a large amount of value in the later years. In the strongest modification ($M^{deg} = 6e6$), the battery survives 15 years and the cumulative Net Present Value (NPV) is $\$1,644,000$. This is an increase of $\$439,000$ in NPV over External Degradation, i.e. an 88.7% recovery of the NPV lost ($\$495,000$) from cycle degradation.

With $M_{deg} = 1 \times 10^6$ the battery only survived partially into its 15^{th} year and only recovers 37.5% of the value lost from cycle degradation. Higher M_{deg} may result in large profits by allowing the battery to survive the 16^{th} year, but our pricing data only lasted 15 years so this was not tested.

We can also characterize this improvement through the investment's internal return rate of return (IRR). For External Degradation, the IRR is 8.5%. For Internal Degradation, this raises to 9.15%.

In a more economically realistic analysis, M_{deg} should be chosen with consideration to the cost of the BESS. For example, if the BESS has no cost (and has no cost to set up), then $M_{deg} = 0$ would be appropriate because the battery could be replaced for free. M_{deg} higher than $6e6$ is likely appropriate. This would yield a larger increase in IRR given the realistic initial investment.

It should be noted that the death cutoff will vary by battery. Nonetheless, death will still occur later in the optimized case and value will still be received. For example, if death is taken at 70% nominal capacity, we still obtain nearly an additional year of value with Internal Degradation. In general, this value decreases as the death cutoff increases.

To get a sense of how realistic these results are in practice (since we have assumed perfect forecasting), note that all three scenarios (internal and external degradation) compared assumed perfect price forecasting. Furthermore, all scenarios compared assumed perfect knowledge of the expected value of the regulation signal. Thus we believe that the largest assumption to worry about is that of perfect knowledge of the variance of the regulation signal. Though fair estimates are possible in practice, less accurate signal variances will lead to errors in the degradation model. This will make the internal degradation LP think that it will degrade the battery with a slightly higher or lower rate than it actually does. However, since perfect forecasting yields absolute errors of this kind on the order of 1e-5 (each hour), we believe that slight increases in this error will not lead to significantly worse results.

D. Heuristics and Parameter Estimation

A heuristic for SoH preservation can be inferred from the decision variables chosen by the modified LP. The primary observation is that many potential regulation awards have been rejected completely. As illustrated in Figure 8, this occurs when the variance of the regulation signal is high relative to the profit of providing the corresponding service. The other regulation variable is not cut simultaneously, so a small change in SoC occurs during these hours. These differences are compensated by a short series of small charge/discharge variables which take the SoC back to the boundaries of $\mathcal{I}$. This heuristic can be appended to the list of heuristics described in section IV-D to form a fairly realistic short horizon optimization scheme. This will be tested in future work.

In order to use the approximation of cycle degradation with accuracy, the DoD function parameters must be known accurately. Instead of finding these experimentally, the linear approximation itself can be used to estimate a_1, a_2, and k simultaneously by measuring the SoH of the battery and updating them from this measurement. This will also be considered in future work.

We will also test the heuristics of subsection IV-D in future work at the same time that we test the regulation heuristics and parameter estimation approach.

This article has been accepted for publication in a future issue of this journal, but has not been fully edited. Content may change prior to final publication. Citation information: DOI 10.1109/TSG.2017.2695196, IEEE Transactions on Smart Grid

E. Optimal R

Reference [6] found that, without degradation considerations, the most valuable power to energy ratio, $P_{max} \cdot (1\ hr.)/E_{max}$ (nominal) for wholesale market is $\frac{1}{2}$ because of the increased cost of BESS with higher ratios (i.e. more state of the art in terms of this ratio). The gap jumping property further establishes this optimal ratio. Larger $P_{max} \cdot (1\ hr.)/E_{max}$ will mean that the initial R is larger. With larger R, larger macro cycles will occur, and therefore more degradation. Thus the increased investment in increasing $P_{max} \cdot (1\ hr.)/E_{max}$ will decay more quickly than the investment up to just $P_{max} \cdot (1\ hr.)/E_{max} = \frac{1}{2}$.

VII. Conclusion

This paper developed a framework for Battery Energy Storage Valuation that is co-optimized with a realistic degradation model. First, BESS optimization was described in detail and a procedure for calculating degradation external to the optimization was explained. It was shown that cycle degradation incurs a 29.1% loss in battery value compared to estimates that did not include it. Properties of the optimized output decisions were then analyzed and a possible heuristic optimization program was discussed. A linear approximation to the degradation function was developed from these properties. By placing the linear model internal to the optimization problem, an additional year of battery lifetime was obtained. This extended lifetime recovered more than 85% of the lost value, reducing the value lost by cycle degradation to just 3.3%. Heuristics for degradation reduction were inferred from the output decision variables of the internal optimization procedure, and an optimal power ratio was argued from the stance of degradation.

Appendix

Proof of Proposition 1.

Summing (6) and (11) yields (59). Summing (7) and (10) yields (60)

$$r_t^d + r_t^u \leq E_{max}/(1\ hr.) - (S_t/(1\ hr.) - P_{max}) \quad (59)$$

$$r_t^d + r_t^u \leq S_t/(1\ hr.) + P_{max} \quad (60)$$

summing (59) and (60) and dividing by 2 then yields

$$r_t^d + r_t^u \leq E_{max}/(2\ hrs.) + P_{max} \quad (61)$$

which is the proposed bound.

To show that this bound is achievable iff. S_t is in the proposed region, we must consider two cases.

First, suppose $P_{max} \leq E_{max}/(2\ hrs.)$ (the typical case in practice). Then if $S_t < P_{max} \cdot (1\ hr.)$, the right hand side of (60) is less than $2P_{max}$ which is less than or equal to $E_{max}/(2\ hrs.) + P_{max}$ so $r_t^u + r_t^d$ cannot meet the proposed bound. If $S_t > E_{max} - P_{max}$, however, the right hand side of (59) again becomes less than $2P_{max}$. Thus the bound (61) cannot be achieved outside of $\mathcal{I}$. Within $\mathcal{I}$, however, the right hand sides of both (59) and (60) are larger than the proposed bound.

Similar logic holds for the case where $P_{max} > E_{max}/(2\ hrs.)$. If $S_t > P_{max} \cdot (1\ hr.)$, the right hand side of (59) becomes E_{max} which is less than $E_{max}/(2\ hrs.) + P_{max}$, and if $S_t < E_{max} - P_{max}$, the right hand side of (60) becomes E_{max}. Again, both right hand sides are larger than the proposed bound when $S_t \in \mathcal{I}$.

This completes the proof. □

References

[1] G. Huff, A. B. Currier, B. C. Kaun, D. M. Rastler, S. B. Chen, D. T. Bradshaw, and W. D. Gauntlett, "DOE/EPRI 2013 electricity storage handbook in collaboration with NRECA," *Report SAND2013*, p. 340, July 2013.

[2] A. Nottrott, J. Kleissl, and B. Washom, "Energy dispatch schedule optimization and cost benefit analysis for grid-connected, photovoltaic-battery storage systems," *Renewable Energy*, vol. 55, pp. 230–240, 2013.

[3] R. K. Lam, D. H. Tran, and H.-g. Yeh, "Economics of residential energy arbitrage in California using a PV system with directly connected energy storage," in *Green Energy and Systems Conference*, 2015, pp. 67–70.

[4] M. D. Anderson and D. S. Carr, "Battery energy storage technologies," *Proceedings of the IEEE*, vol. 81, no. 3, pp. 475–479, 1993.

[5] A. Oudalov, D. Chartouni, and C. Ohler, "Optimizing a battery energy storage system for primary frequency control," *IEEE Transactions on Power Systems*, vol. 22, no. 3, pp. 1259–1266, 2007.

[6] N. Yu and B. Foggo, "Stochastic valuation of energy storage in wholesale power markets," submitted to Energy Economics, 2016. [Online]. Available: http://www.ece.ucr.edu/~nyu/2016-Stochastic-Energy-Storage-Valuation.pdf

[7] D. Wu, C. Jin, P. Balducci, and M. Kintner-Meyer, "An energy storage assessment: using optimal control strategies to capture multiple services," *2015 IEEE Power & Energy Society General Meeting*, pp. 1–5, 2015.

[8] S. Bashash, S. Moura, and H. Fathy, "Charge trajectory optimization of plug-in hybrid electric vehicles for energy cost reduction and battery health enhancement," *American Control Conference (ACC), 2010*, pp. 5824–5831, 2010.

[9] M. Ecker, N. Nieto, S. Kabitz, J. Schmalstieg, H. Blanke, A. Warnecke, and D. U. Sauer, "Calendar and cycle life study of Li(NiMnCo)O2-based 18650 lithium-ion batteries," *Journal of Power Sources*, vol. 248, pp. 839–851, 2014. [Online]. Available: http://dx.doi.org/10.1016/j.jpowsour.2013.09.143

[10] J. Shen, S. Dusmez, and A. Khaligh, "Optimization of sizing and battery cycle life in battery/ultracapacitor hybrid energy storage systems for electric vehicle applications," *Industrial Informatics, IEEE Transactions on*, vol. 10, no. 4, pp. 2112–2121, 2014.

[11] A. Hoke, A. Brissette, K. Smith, A. Pratt, and D. Maksimovic, "Accounting for lithium-ion battery degradation in electric vehicle charging Optimization," *IEEE Journal of Emerging and Selected Topics in Power Electronics*, vol. 2, no. 3, pp. 691–700, 2014.

[12] A. Rajabi-Ghahnavieh and A.-S. Hamedi, "Explicit degradation modeling in optimal lead-acid battery use for photovoltaic systems," *IET Generation, Transmission & Distribution*, vol. 10, no. 4, pp. 1098–1106, 2016.

[13] V. Muenzel, M. Brazil, V. Muenzel, J. D. Hoog, and M. Brazil, "A multi-factor battery cycle life prediction methodology for optimal battery management," in *Proceedings of the 2015 ACM Sixth International Conference on Future Energy Systems*, January 2015, pp. 57–66.

[14] T. Cui, S. Chen, Y. Wang, Q. Zhu, S. Nazarian, and M. Pedram, "Optimal co-scheduling of HVAC control and battery management for energy-efficient buildings considering state-of-health degradation," *20th Asia and South Pacific Design Automation Conference, ASP-DAC 2015*, pp. 775–780, 2016.

[15] B. Zhao, X. Zhang, J. Chen, C. Wang, and L. Guo, "Operation optimization of standalone microgrids considering lifetime characteristics of battery energy storage system," *IEEE Transactions on Sustainable Energy*, vol. 4, no. 4, pp. 934–943, 2013.

[16] P. Fortenbacher, J. L. Mathieu, and G. Andersson, "Modeling, identification, and optimal control of batteries for power system applications," *2014 Power Systems Computation Conference*, pp. 1–7, 2014. [Online]. Available: http://ieeexplore.ieee.org/lpdocs/epic03/wrapper.htm?arnumber=7038360

[17] J. L. Mathieu and J. A. Taylor, "Controlling nonlinearbatteries for power systems : trading off performance and battery life," in *Power Systems Computation Conference*.

[18] G. He, Q. Chen, C. Kang, P. Pinson, and Q. Xia, "Optimal bidding strategy of battery storage in power markets considering performance-based regulation and battery cycle life," *IEEE Transactions on Smart Grid*, pp. 2359–2367, 2016.

[19] "Replication data for: battery storage valuation with optimal degradation - harvard dataverse." [Online]. Available: https://dataverse.harvard.edu/dataset.xhtml?persistentId=doi:10.7910/DVN/KDHAJY

[20] B. Xu, A. Oudalov, A. Ulbig, G. Andersson, and D. Kirschen, "Modeling of lithium-ion battery degradation for cell life assessment," *IEEE Transactions on Smart Grid*, vol. PP, no. 99, pp. 1–1, 2016.

[21] "PJM-Ancillary Services." [Online]. Available: http://www.pjm.com/markets-and-operations/ancillary-services.aspx

[22] C. Amzallag, J. P. Gerey, J. L. Robert, and J. Bahuaud, "Standardization of the rainflow counting method for fatigue analysis," *International Journal of Fatigue*, vol. 16, no. 4, pp. 287–293, 1994.

[23] J. Vetter, P. Novak, M. R. Wagner, C. Veit, K. C. Moller, J. O. Besenhard, M. Winter, M. Wohlfahrt-Mehrens, C. Vogler, and A. Hammouche, "Ageing mechanisms in lithium-ion batteries," *Journal of Power Sources*, vol. 147, no. 1-2, pp. 269–281, 2005.

[24] D. Simmons, "Conditional measures and conditional expectation; Rohlin's disintegration theorem," *Discrete and Continuous Dynamical Systems*, vol. 32, no. 7, pp. 2565–2582, 2012.

[25] E. Engel and R. M. Dreizler, *Density functional theory: an advanced course*, 2011, vol. 2011.

[26] R. P. Hafen, V. V. Vishwanathan, K. Subbarao, and M. C. Kintner-Meyer, "Requirements for defining utility drive cycles: an exploratory analysis of grid frequency regulation data for establishing battery performance testing standards," October 2011. [Online]. Available: http://www.osti.gov/energycitations/servlets/purl/1028571/$\backslash$nhttp://www.pnnl.gov/main/publications/external/technical{_}reports/PNNL-20849.pdf